



Bayero Journal of Pure and Applied Sciences, 15(1): 169 - 180

Received: March, 2022

Accepted: April, 2022

ISSN 2006 – 6996

KINETIC AND THERMODYNAMIC STUDIES OF ADSORPTION OF LEAD (II) IONS ON MAGNETITE, BAOBAB (*Adansonia digitata*) AND MAGNETITE - BAOBAB COMPOSITE

Abdus-Salam, N., Adekola, S.K. and Bello, M.O.*

Department of Chemistry, University of Ilorin, P.M.B. 1515, Ilorin, Kwara State, Nigeria

*Corresponding Author E-mail address: bello.mo@unilorin.edu.ng

ABSTRACT

The detrimental consequences of excessive levels of heavy metal contamination on living things served as the motivation for this study. Adsorption of Pb(II) ions was investigated on synthetic magnetite (MG), baobab fruit shell (BB) and magnetite-baobab composite (MB). The batch equilibrium technique was used to investigate the adsorption of Pb(II) ions. The effects of initial metal concentrations (15-500 mg/L), adsorbent dose (0.05-0.3 g), contact time (5-150 min), pH (2-8) and temperature (303-343 K) on the adsorption capacity of the adsorbent were studied. Langmuir, Freundlich and Temkin isotherms were used to describe the adsorption of Pb(II) ions. The maximum adsorption capacity, q_{max} of MB, MG and BB was 249.86, 227.45 and 34.67 mg/g respectively at a concentration of 500 mg/L of Pb(II) ions. Freundlich model was shown to have the best fit for the adsorption data in the following order: BB > MG > MB, with R^2 values of 0.9954, 0.980 and 0.9797 respectively. Freundlich adsorption intensity for MG, BB and MB are 1.590, 1.339 and 1.761 respectively. The kinetic and thermodynamic investigations revealed that the adsorption followed pseudo-second-order kinetics and endothermic process. The amount of Pb(II) ions adsorbed after each stage of the desorption process varied between the different acid concentrations, according to sorption-desorption studies using spent adsorbents. The highest stepwise adsorptions of Pb(II) ions were observed when 0.5 M HCl was utilized as a stripping agent for BB while 0.1 M HCl favoured MG and MB.

Keywords: Adsorption, baobab; biosorbent; isotherm; kinetic model; composite

INTRODUCTION

The dramatic increase in industrial and mining operations has caused different ecological degradations, posing risks to human health and the environment (Foo & Hammed, 2010). Heavy metals are found naturally in the earth's crust (Tchounwou et al., 2012) and cannot be degraded. They get into our bodies in minute amounts from food, water and air. Some heavy metals (such as copper, selenium and zinc) are necessary for human metabolism as trace elements. They can, however, cause toxicity at large concentrations. Drinking contaminated water (e.g., through lead pipes), breathing high ambient air concentrations near emission sources, or ingesting heavy metals through the food chain can all cause heavy metal poisoning (Sani, 2011). Heavy metals are hazardous because they bioaccumulate in bodily tissues for no apparent purpose (Salami and Adekola, 2002). Lead has the potential to affect not only the microbial communities but also the groundwater and hence, has a toxicological impact on human health. Pb(II) ions have the

potential to accumulate in organisms, causing numerous diseases and disorders in the nervous system, kidneys and reproductive system, particularly in children (Salami and Adekola, 2002). Effluents containing heavy metals are often discharged from several industrial processes with little or no treatment (Bisht et al 2016; Bhamare et al., 2021) into the environmental domains. The extent of pollution and its health effect on organisms in the environment depends on the quantity and nature of the heavy metals discharged. It was reported that the toxicity from annual heavy metal discharge is worse than the combined toxicity effects of radioactive and organic waste discharge (Abdus-Salam and Adekola, 2005). The common methods of heavy metal removal are ion exchange, biochemical treatment, chemical precipitation, ultra-filtration and adsorption (Abdus-Salam and Bello, 2015). Adsorption is a cost-effective and environmentally friendly method for removing heavy metal ions from aqueous solutions (Chakraborty et al., 2020; Abas et al., 2013).

For the removal of heavy metal ions by adsorption, various adsorbents have been used, including activated carbon (Alhamed and Bamufleh, 2009), termite mound clay (Abdus-Salam and Bello, 2015), zeolites (Hedstrom, 2001; Wang and Peng, 2010), resins (Chao et al., 2014), biosorbents (Crini, 2006), hydrogel (Wang et al., 2012) among others. To improve the performance of some of the adsorbent materials that have been widely applied as low-cost adsorbents, this present study focused on composite materials. Composite preparation is a fast-growing area (Abdus-Salam and Ikudaisi, 2017) that can also be applied in water treatment especially when low-cost materials are employed. Consequently, this research used magnetite (MG), baobab (BB) and magnetite-baobab composite (MB) for the removal of Pb(II) ions from aqueous solutions.

MATERIALS AND METHODS

Sample Collection and Preparation

The baobab fruit shells (BB) were obtained within the environment of the University of Ilorin, Ilorin, Kwara State, Nigeria and were rinsed with distilled water to remove impurities deposited on it. The BB was air-dried and then oven-dried at 80 °C to constant mass. The dried shells were pulverised and sieved to obtain particle sizes $\leq 300 \mu\text{m}$. The baobab shell powder was soaked in 0.1 M HNO_3 (67-70%) for 24 hr. The mixture was filtered and the powder residue was washed with distilled water several times until pH of the filtrate was tested neutral. It was then air-dried at ambient temperature, pulverised and sieved below 90 μm . The magnetite (MG) and Magnetic-Baobab (MB) composite used herein were previously synthesized (Abdus-Salam and Adekola, 2018). All reagents used were of analytical grade (BDH).

Batch Adsorption Experiment

The batch adsorption experiment was carried in 100 mL conical flasks as reactors and each adsorbent (MG, BB and MB) was separately mixed with 25 mL of Pb(II) ions. The mixture in the reactors was equilibrated on a thermostatic motorized orbital mechanical shaker (SHA-B Water Temperature Oscillator). At equilibrium, the supernatant liquids were filtered and the un-adsorbed Pb(II) ions in the filtrate were analysed by atomic absorption spectrophotometry (AAS) (Abdus-Salam and Adekola, 2018). The quantities of Pb(II) ions adsorbed by the adsorbents were calculated using eqn. 1 (Chen et al., 2010; Adekola et al., 2011).

$$q_e = \frac{C_0 - C_f}{M} \times V \quad (1)$$

The percentage removal (% R_{em}) by the adsorbents was expressed as (Abia and Asuquo, 2006):

$$\% \text{ rem} = \frac{(C_0 - C_f)}{C_0} \times 100 \quad (2)$$

Where q_e is the quantity of Pb(II) ions adsorbed (mg/g), C_0 and C_f are the initial and final concentrations of Pb(II) ions in solution at any time (mg/L) and V is the total volume in the flask (L) and M is the mass of adsorbent used (g).

Optimisation of Adsorption Parameters

Effect of Initial Pb(II) Ion Concentration

A 25 mL of varying concentrations (15, 25, 75, 150, 350 and 500 mg/L) of Pb(II) ions solutions were contacted with 0.1 g of MG, BB and MB at 30 °C and agitated separately on a mechanical shaker for 5 hr. The mixtures were then filtered and the filtrates were analysed for un-adsorbed Pb(II) ions using AAS (Jimoh et al., 2012). The quantities adsorbed, q_e , were calculated using eqn. 1.

Effect of Adsorbate and Adsorbent Contact Time

A 0.1 g of MG, BB and MB was weighed into nine sets of 100 mL conical flasks for each adsorbent and mixed with 25 mL of the optimum concentration (500 mg/L) of Pb (II) ions. Each set of the adsorbent-adsorbate mixtures was agitated for 5, 10, 15, 30, 45, 60, 90, 120 and 150 min time intervals. At the expiration of each time interval, the mixtures were filtered and the filtrates were analysed for Pb(II) ions using AAS. The quantities adsorbed were calculated using eqn. 1.

Effect of Adsorbent Dosage

A 25 mL of 500 mg/L Pb(II) ions that gave optimal adsorption per 0.1 g MG, BB and MB composite was separately contacted with varying amounts (0.1, 0.5, 1.0, 1.5 and 2.0 g) of MG for 5 min, BB for 120 min and MB for 90 min at 30 °C. The mixtures were agitated on a thermostatic orbital mechanical shaker. At the completion of the contact time, the solutions were filtered and the filtrates were analysed for Pb(II) using AAS. The quantities adsorbed, q_e , were calculated using eqn. 1.

Effect of Temperature

A 25 mL of the optimum concentration (500 mg/L) of Pb(II) ions was contacted with 0.05 g of MG for 5 min, 0.1 g of BB for 120 min and 0.05 g of MB for 90 min in 100 mL conical flasks. The mixtures were agitated at a temperature range between 30 and 70 °C (30, 40, 50, 60 and 70 °C). The flasks were brought out and filtered at the end of each reaction time. The filtrates were analysed for Pb(II) ions using AAS and the quantities adsorbed were calculated using eqn. 1.

Effect of pH

The effect of pH on the adsorption of Pb(II) ions was carried out over a pH range of 2 to 8. A 25 mL of the optimum concentration (500 mg/L) of Pb(II) ions was contacted with 0.05 g of MG for 5 min, 0.05 g of MB for 90 min and 0.1 g of BB for 120 min in 100 mL conical flasks. The mixtures were equilibrated at a constant temperature of 70 °C and filtered at the end of their respective contact time. The filtrates were analysed for Pb(II) ions using AAS and the quantities adsorbed were calculated using eqn. 1.

Sorption-Desorption Experiment

A three steps sorption-desorption process was done by following the method reported by Abdus-Salam and Itiola (2012) using different concentrations (0.1-2.0 M) of HCl as stripping agents.

Adsorption Isotherm

Three isotherm models; Langmuir, Freundlich and Temkin were used to evaluate the equilibrium adsorption data of Pb(II) ions onto the adsorbents for further understanding of the process.

Table 1: Isotherm equations

Isotherm model	Equation	Plot	Reference
Langmuir	$\frac{C_e}{q_e} = \frac{1}{q_m K_L} + \frac{C_e}{q_m}$ $R_L = \frac{1}{1 + K_L C_o}$	$\frac{C_e}{q_e}$ vs C_e	(Chen, 2015)
Freundlich	$\log q_e = \log K_f + \frac{1}{n} \log C_e$	$\log q_e$ vs $\log C_e$	(Bello et al., 2021)
Temkin	$q_e = \beta \ln A_T + \beta \ln C_e$ $\beta = \frac{RT}{b}$	q_e vs $\ln C_e$	(Inyinbor et al., 2016)

Where q_e is the amount of Pb(II) ions adsorbed (mg/g); C_e is the equilibrium concentration (mg/L); q_m is the monolayer adsorption capacity (mg/g); K_L is the Langmuir constant (L/mg); R_L is a dimensionless constant separation factor; K_f is the Freundlich constant (mg/g) and n is the empirical parameter which is related to the sorption intensity, A_T is the equilibrium binding constant (L/mg) corresponding to the maximum binding energy; β is related to the heat of adsorption (J/mol); b is Temkin isotherm constant (J/mol); T is temperature (273 K) and R is gas constant (8.314 J/mol.K).

Adsorption Kinetics

The adsorption kinetics were investigated using pseudo-first-order and pseudo-second-order models.

Table 2: Kinetic equations

Kinetic model	Equation	Plot	Reference
Pseudo-first-order	$\log(q_e - q_t) = \log q_e - \frac{k_1}{2.303} t$	$\log(q_e - q_t)$ vs t	(Ho and McKay, 1998)
Pseudo-second-order	$\frac{t}{q_t} = \frac{1}{K_2 q_e^2} + \frac{1}{q_e} t$	$\frac{t}{q_t}$ vs t	(Ho and McKay, 1999)

Where q_e and q_t are the amounts of Pb(II) ions adsorbed (mg/g) at equilibrium and at time t (min), respectively; k_1 (min^{-1}) is the adsorption rate constant for pseudo-first-order and k_2 (g/mg.min) is the pseudo-second-order rate constant.

Adsorption Thermodynamics

The thermodynamic equations in Table 3 were applied to the data obtained from the effect of temperature on the adsorption process. The

thermodynamic parameters such as changes in Gibbs free energy (ΔG), enthalpy (ΔH) and entropy (ΔS) were determined from the equations.

Table 3: Thermodynamic equations

Model	Equation	Plot	Reference
Van't Hoff	$\ln k_c = -\frac{\Delta H^0}{RT} + \frac{\Delta S^0}{R}$ $k_c = \frac{C_{ads}}{C_e}$ $\Delta G^0 = \Delta H^0 - T\Delta S^0$	$\ln k_c$ vs $\frac{1}{T}$	(Abdus-Salam and Adekola, 2018)

Where K_c is the equilibrium constant; C_e and C_{ads} are the concentration of Pb(II) ions in solution and on adsorbent at equilibrium respectively (mg/L). ΔG^0 , ΔH^0 and ΔS^0 are changed in Gibbs free energy (kJ/mol), enthalpy (kJ/mol) and entropy (J/mol.K) respectively; R is the gas constant (8.314 J/mol.K) and T is the temperature (K).

RESULTS AND DISCUSSION

Adsorption Experiment

Effect of Initial Concentration

The quantity of Pb(II) ions adsorbed per gram of MG, BB and MB increased with increasing initial concentration as shown in Fig. 1. High concentrations result in a corresponding increase in driving force, which improves the interaction between the metal ions in the aqueous phase and the active sites of the adsorbents. At low concentrations, the available driving force that is required to transfer the metal ions onto the

adsorbent particles is low. As a result of this, there was an increase in the uptake of Pb(II) ions at higher concentrations. Similar results were obtained in the adsorption of Cu and Fe ions from aqueous solutions using pine fruit as an adsorbent (Najim et al., 2008). Relatively, MB exhibited a higher adsorption capacity (123.92 mg/g) for Pb(II) ions compared to MG (90.94 mg/g) and BB (25.69 mg/g). Therefore, the adsorption capacity of the three adsorbents for Pb(II) ions is in the order of MB>MG>BB.

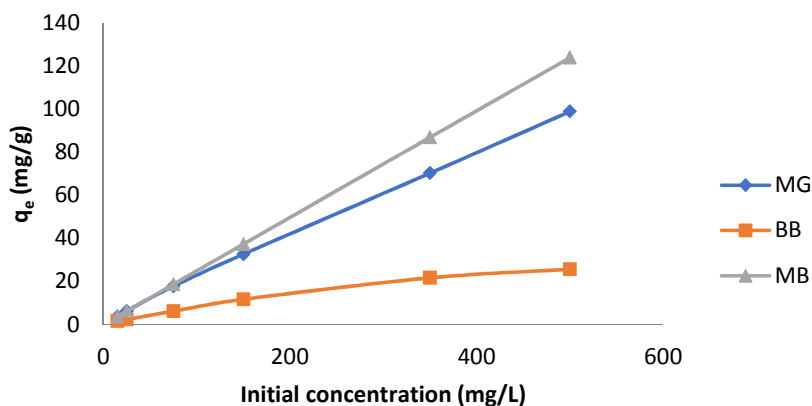


Figure 1: Effect of concentration on adsorption of Pb(II) ions onto BB, MG and MB

Effect of Adsorbate and Adsorbent Contact Time

Magnetite (MG) showed rapid adsorption and attaining maximum within 5 min of contact time due to the easy accessibility of the adsorption sites by Pb(II) ions (Fig. not shown). The rate of adsorption indicated that the removal of 85.13% (106.42 mg/g) of Pb(II) ions was accomplished within the first 5 min. Iron oxides as adsorbents are known for fast kinetics and attaining equilibrium within a short contact time (Giraldo and Moreno-pirajan, 2013; Khodabakhshi et al., 2011). Furthermore, the rapid adsorption of Pb(II) ions by MG can be attributed to the external surface adsorption which is different from the microporous adsorption process which facilitates access to the active sites and resulted in a rapid approach to equilibrium (Chowdhury, 2013). Rapid adsorption of metal ions during the initial stage was due to the large initial concentration gradient between the adsorbate in solution and the number of available vacant sites on the adsorbent surface (Chigondo et al., 2013).

The MB and BB curves rose slowly and steadily until equilibrium was attained at 90 and 120 min (Fig. not shown) with a maximum adsorption capacity of 109.10 mg/g and 28.69 mg/g respectively. After this equilibrium time, Pb(II)

ions adsorption became practically the same. A similar trend was observed from the adsorption of Pb(II) ion onto kaolinite clay as a function of contact times (Orumwense, 1996). Constant adsorption is an indication of equilibration due to the saturation of adsorption sites.

Effect of Adsorbent Dosage

It was observed that the percentage of Pb(II) ions adsorbed increased as the adsorbent dosage increased from 0.05 to 0.30 g but the amount adsorbed per unit mass of the adsorbent decreased considerably for MG, BB and MB (Fig. not shown). The decrease in adsorption per unit mass with an increasing dose of adsorbent is attributed to a possible overlapping of adsorption sites as the adsorbent dose increases or clogging of adsorbent which will equally reduce the effective adsorption sites (Senthil Kumar et al., 2010). As the adsorbents dose increased from 0.05 to 0.3 g, the quantity of Pb(II) ions adsorbed (mg/g) decreased from 121.05 to 35.84 mg/g on MG, 29.09 to 16.86 mg/g on BB and 131.98 to 41.38 mg/g on MB. This is an indication that a low adsorbent dosage has a high adsorption capacity for Pb(II) ions, especially MG and MB. This was the trend observed in similar research (Kaya et al., 2009; Abdus-Salam and Adekola, 2005).

Effect of Temperature

Figure 2 shows the effect of temperature on the adsorption of Pb(II) ions on BB, MG and MB. An increase in the adsorption capacities with an increase in temperature was observed especially for MG and MB. This observation suggests that the adsorption process is endothermic. For ions to be adsorbed on the adsorbents, hydrated ions have to lose their hydrated shell, and this dehydration process needs energy which is

compensated for by the increase in temperature (Babarinde and Babalola, 2010; Castaldi et al., 2008). The removal of water molecules from hydrated ions is essentially an endothermic process. This increase in the quantity of Pb(II) ions adsorbed was probably due to an increase in the energy of the solution with increasing temperature which stimulated the diffusion of Pb(II) ions onto the adsorbents particles' surface.

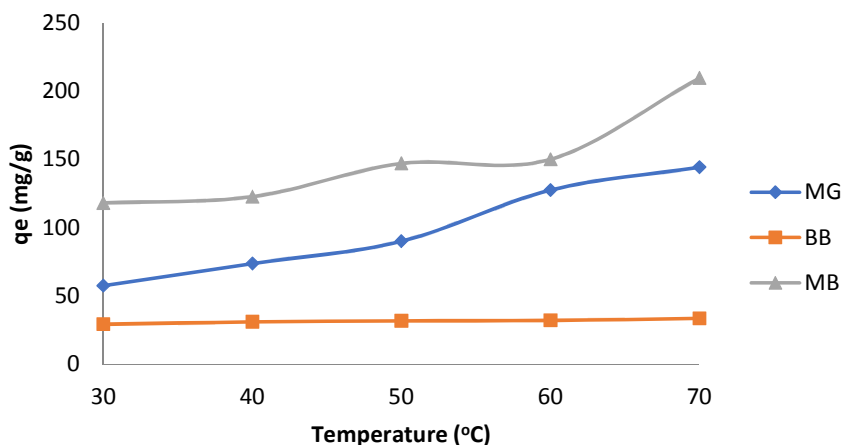


Figure 2. Effect of temperature on the adsorption of Pb(II) ions onto BB, MG and MB

Effect of pH

From Fig. 3, it was observed that the amount of Pb(II) ions adsorbed from aqueous solution was low at lower pH values and increased with increasing initial pH of the solution for all adsorbents. At pH of 8.0, 249.86 mg/g of Pb(II) ions were adsorbed compared to 165.32 mg/g adsorbed at pH of 2.0 on MB which represents 90.98% and 63.53% adsorption respectively. Also, it was observed that the maximum adsorption of Pb(II) ions on MG and MB adsorbents occurred within the pH range of 6 – 8. An increase in adsorption with pH increase may be due to the variation of surface charge of MG and MB as a function of the pH of the solution. The dependence of metal ions sorption on pH is related to both the surface functional groups of the adsorbent and the metal ion chemistry in the solution (Wang and Xing, 2002) which gave rise to S-like curves. The maximum Pb(II) ions adsorption was achieved at pH 6 and above this pH, the removal the ions was almost constant. This may be a result of saturation of active adsorption sites and/or the formation of a soluble metal hydroxide, $Pb(OH)_2$ which is favourable at alkaline pH (Zvinowanda et al., 2009; Wang and Xing, 2002; Bayat, 2002). A

similar observation was made on the sorption of Pb(II) and Cu(II) ions onto magnetite eggshells- Fe_3O_4 powder (Ren et al., 2012) and Pt^{2+} and Au^{3+} ions from aqueous solutions by magnetite nanoparticles (Giraldo and Moreno-pirajan, 2013).

The initial increase in the adsorption capacity with an increase in pH was attributed to a decrease in competition between hydrogen ions and Pb(II) ions for the active sites on the adsorbents and also to a decrease in positive surface charge. As the pH increases, a more negatively charged surface becomes available and thereby facilitated greater metal adsorption. Metal ions are more soluble at lower pH values and this reduces the chances of their adsorption (Onundi et al., 2010). Furthermore, at lower pH, the surface of the adsorbent is surrounded by hydrogen ions (H^+) thereby blocking metal ions from active binding sites (Mohammed et al., 2013). An increase in the pH of the adsorbing medium creates more negative charges on the adsorbent surface, which favours the adsorption of positively charged species (Abdus-Salam and Adekola, 2005; Kadirvelu and Namasivayam, 2003).

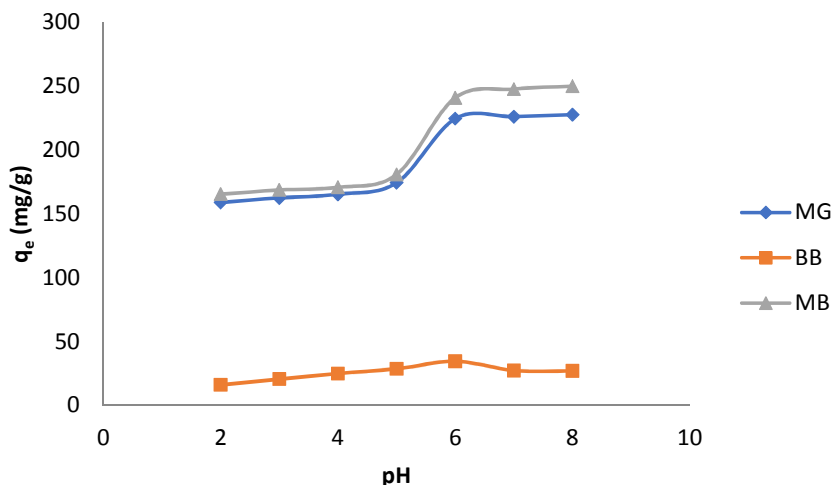


Figure 3. Effect of pH on adsorption of Pb(II) ions onto BB, MG and MB

Adsorption Isotherm

The adsorption isotherm is a graphical description of how adsorbates interact with adsorbents which is highly important in the optimization of adsorbents usage (Bulut and Aydin, 2005).

Langmuir Isotherm

It can be deduced from the plots (Fig. not shown) using the correlation coefficient (R^2) values that the experimental data for the MB best fitted into the model with 0.999 followed by that of BB with 0.975 and MG with 0.881 for Pb(II) ion. The applicability of the Langmuir isotherm indicates good monolayer coverage of Pb(II) ions on the surface of MG, BB and MB which suggests the formation of a monolayer on the adsorbent surface in the given concentration range (Alli and Muhammad, 2008). The Langmuir isotherm constants are reported in Table 4.

The calculated values of the separation factor, R_L are within the range $0 < R_L < 1$ (Tables 4) and it

is an indication that the adsorption of Pb(II) ions onto the three adsorbents is favourable for the concentrations considered.

Freundlich Isotherm

The isotherm yielded good linear plots (Fig. 4) and Freundlich adsorption intensity, n , for MG, BB and MB are 1.590, 1.339 and 1.761 respectively. The n value predicts whether the adsorption of a given ion is favourable or not. Since $n > 1$ for adsorption of Pb(II) ions, the adsorption intensity is favourable at higher concentrations (Adekola et al., 2011). Comparing the R^2 values for the adsorption of Pb(II) ions on the adsorbents, the best fittings of data are in the descending order: BB > MG > MB (i.e. $0.9954 > 0.980 > 0.9797$). A good fit of experimental data to the Freundlich model suggests that there are heterogeneous sites on the adsorbents with different energy values for adsorption of Pb(II) ions.

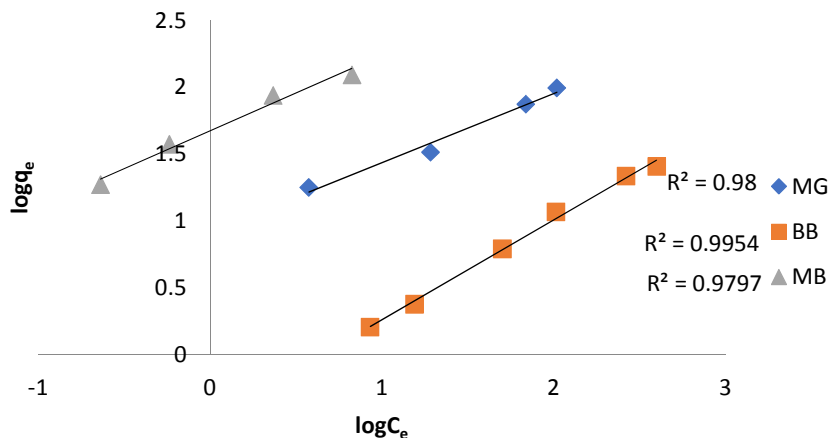


Fig. 4. Freundlich adsorption isotherm for Pb(II) ions

Temkin Isotherm

A plot of q_e against $\ln C_e$ represents the Temkin isotherm behaviour for the adsorption of Pb(II) on MG, BB and MB (Fig. not shown) and from which the Temkin constants were derived (Table 4). The correlation coefficient (R^2) values for Pb(II) ions on MB, BB and MG are 0.990, 0.925 and 0.896 respectively. The Temkin adsorption equilibrium binding energy constant, A_T , for MG,

BB and MB are 0.9735, 0.095 and 6.75 L/mg respectively. This indicates that MB has a higher potential for adsorbent-metal ion interaction followed by MG while BB has the least potential. The low A_T value for BB suggests that there is an indirect interaction among the particles of adsorbents and adsorbates which corresponds to the linear decrease in the heat of adsorption of all the molecules in the layer.

Table 4: Isotherm parameters for the adsorption of Pb(II) ions onto MG, BB and MB

Model	Parameter	Adsorbent		
		MG	BB	MB
Langmuir	q_m (mg/g)	142.86	43.48	166.67
	K_L (L/mg)	0.023	0.0038	0.545
	R_L	0.084	0.345	0.0037
	R^2	0.881	0.975	0.999
Freundlich	n	1.590	1.339	1.761
	$1/n$	0.629	0.747	0.568
	K_f (mg/g)	5.42	0.327	47.206
	R^2	0.980	0.9954	0.9797
Temkin	β (J/mol)	17.68	-15.02	31.78
	b (J/mol)	140.134	388.334	77.96
	A_T (L/mg)	0.9735	0.095	6.75
	R^2	0.896	0.925	0.990

Adsorption Kinetics

Adsorption kinetics provide information on the residence time of adsorbate at the aqueous-adsorbate interface (Naiya et al., 2009). The R^2 value together with the closeness of the experimental quantity adsorbed ($q_{e, exp.}$) and the calculated values ($q_{e, cal.}$) was used to determine the fitness of the experimental data in a particular kinetics model.

Pseudo-First-Order Kinetic Model

The plot of pseudo-first-order (Fig. not shown) yielded a low correlation coefficient (R^2) value for MG indicating that the experimental data does not fit well the model. It was however applicable to describe the adsorption process of Pb(II) ions onto BB and MB as indicated by their high R^2 values (Table 5).

Pseudo-Second-Order Kinetic Model

Fig. 5 shows the fitness of the adsorption of Pb(II) ions onto the three adsorbents to the linearized form of the pseudo-second-order model and the obtained kinetic parameters are presented in Table 5. The R^2 values are 0.9951, 0.9086 and 0.9998 for MG, BB and MB respectively. Also, the experimental q_e and calculated one are closed in value. This suggests that the adsorption process is better described by the pseudo-second-order model (Giraldo and Moreno-pirajan, 2013; Emadi et al., 2013). Consequently, the main adsorption mechanism probably involves a chemisorption reaction. In chemisorption, heavy metal ions stick to the adsorbent surface forming a chemical (usually covalent) bond at sites that maximise their coordination with the surface (Atkin, 1995).

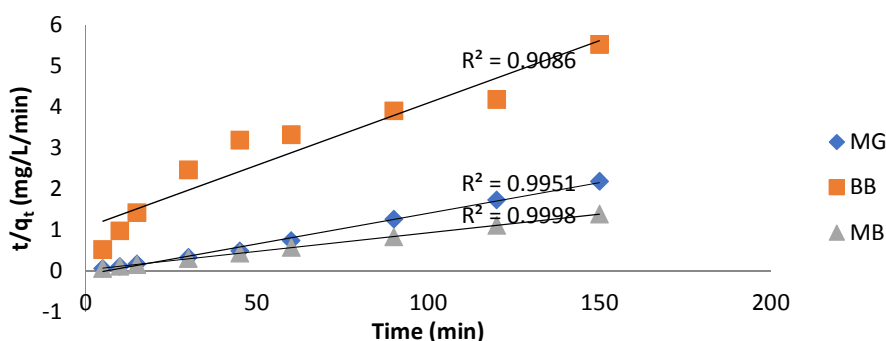


Fig. 5. Pseudo-second-order graph for adsorption of Pb(II) ions

Table 5: Kinetic constants for Pb(II) ions adsorption

Model	Parameter	Adsorbent		
		MG	BB	MB
Pseudo-first-order	k_1 (min^{-1})	1.84×10^{-2}	1.84×10^{-2}	2.07×10^{-2}
	q_e (mg/g)	4.01	26.73	10.94
	R^2	0.633	0.888	0.916
Pseudo-second-order	k_2 (g/mg.min)	2.39×10^{-3}	8.51×10^{-4}	7.36×10^{-3}
	q_e (mg/g)	66.67	33.33	111.11
	R^2	0.9951	0.9086	0.9998

Adsorption Thermodynamics

Fig. 6 shows the Vant Hoff plot of the adsorption data obtained from the effect of temperature and the thermodynamic parameters are summarised in Table 6. The positive values of ΔH for the adsorption of Pb(II) ions onto the three adsorbents vary from 4.27 to 32.78 kJ/mol, indicating that the adsorption processes were physisorption and endothermic. Generally, values of ΔH below 40 kJ/mol are regarded to be physisorption processes (Shikuku et al., 2018) while that of chemisorption is nearly between 80 and 200 kJ/mol (Liu and Liu, 2008). The positive values of ΔS which range from 4.15 to 97.77 J/mol.K for the adsorption of Pb(II) ions onto the adsorbents suggest increased randomness at the adsorbent-adsorbate interface (Jain and Sharma, 2002). The negative

values of ΔG at all temperatures studied for MB suggest spontaneity of the adsorption process. In the case of MG, the reaction becomes more feasible and spontaneous as the temperature was raised to 333K and 343K. Although the adsorption was not spontaneous for BB, the positive value decreased with increasing temperature. This is an indication that the adsorption can be improved upon by increasing the temperature of the adsorption process (Omar and Al-Itaw, 2007). The ΔG values which range from 3.04 to -5.81 kJ/mol further confirm the adsorption processes to be physisorption. Sen et al., (2011) reported that change in free energy (ΔG) for physisorption is in the range of -20 to 0 kJ/mol and that of chemisorption varies between -80 and -400 kJ/mol.

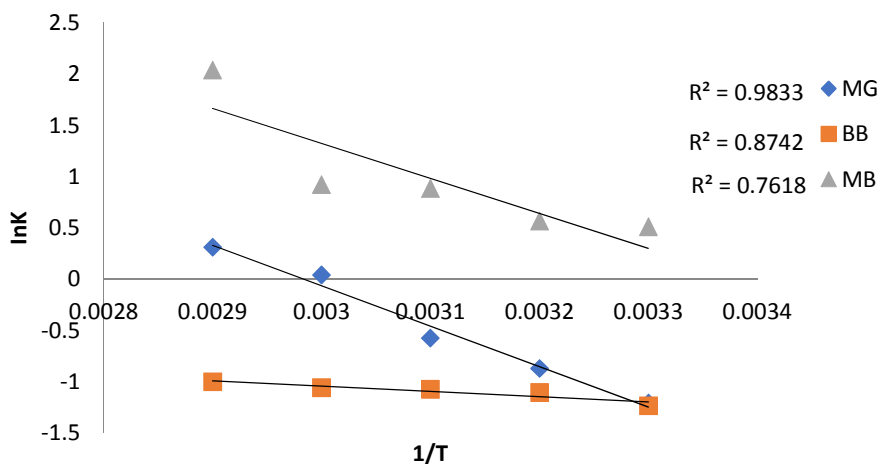


Fig. 6. Van't Hoff graph for Pb(II) ions adsorption at different temperature

Table 6: Thermodynamic parameters for the adsorption of Pb(II) ions

Adsorbent	ΔH (kJ/mol)	ΔS (J/mol.K)	ΔG (kJ/mol)				
			303K	313K	323K	333K	343K
MG	32.78	97.77	3.04	2.26	1.54	-0.11	-0.88
BB	4.27	4.15	3.11	2.87	2.88	2.93	2.85
MB	28.33	95.94	-1.29	-1.47	-2.37	-2.55	-5.81

Desorption

A desorption experiment is usually carried out to determine the life span to which the adsorbents can be put to use (Amer et al., 2009). The data obtained from three steps adsorption-desorption

experiments were plotted. It was observed from the plots (Figs. 7 a-c) that the quantity of Pb(II) ions adsorbed decreased in the successful steps of the adsorption-desorption process.

This might be due to the incomplete desorption of Pb(II) ions and which made some adsorption sites not available during the subsequent adsorption process. The results showed that a significant amount of Pb(II) ions was still adsorbed after the third usage of the adsorbents and there is a great affinity for Pb(II) ions. The highest degree of adsorption of Pb(II) ions on MG and MB was obtained when 0.1 M HCl

stripping agent was used and 0.5 M HCl for BB. The percentage adsorption following first, second and third desorption processes were 78.86%, 71.87% and 67.06% for MG, 80.93%, 73.68% and 68.0% for MB and 68.13%, 63.30% and 53.64% for BB respectively. A similar trend was observed for Pb(II) ions removal by termite mound (Abdus-Salam and Itiola, 2012).

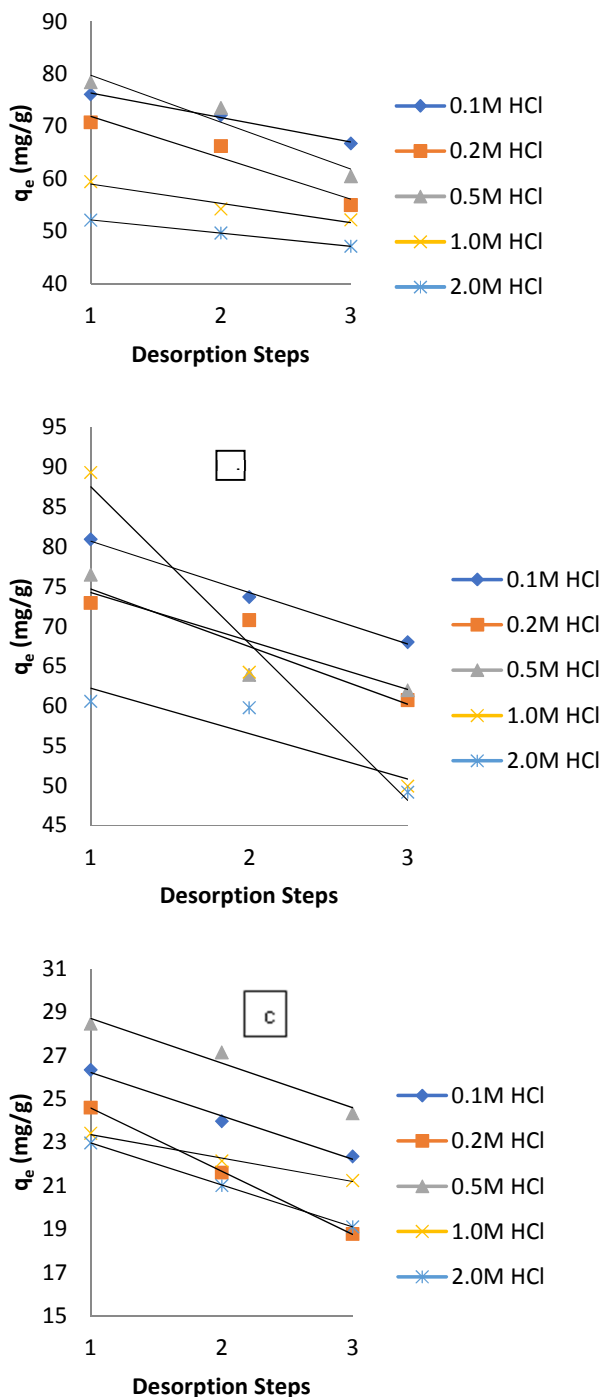


Fig. 7. Quantity of Pb(II) adsorbed (q_e) onto (a) MG (b) MB and (c) BB versus desorption steps for various concentrations of HCl.

CONCLUSION

This study has demonstrated that the synthesized magnetite particles (MG), baobab fruit shells (BB) and magnetite-baobab composite (MB) have favourable properties for the adsorption of Pb(II) ions from aqueous solutions. From the adsorption experiment, Pb(II) ions adsorption efficiency was found to be influenced by initial metal ion concentration, adsorbent dose, contact time, temperature and pH. Although adsorption data were subjected to Langmuir, Freundlich and Temkin isotherm models for a test of fitting, the Freundlich isotherm fitted the experimental data best with

R^2 value of 0.9954, 0.98 and 0.9797 for adsorption of Pb(II) ions on BB, MG and MB respectively. The pseudo-second-order kinetic model best described the adsorption of Pb(II) ions on the adsorbents with R^2 value close to unity suggesting a covalently bonded chemical process. Thermodynamic studies showed that the adsorption processes were endothermic and mostly spontaneous for MG and MB. The three adsorbents have also been found to have high efficiency for re-use at low concentrations of HCl leachant which suggests a good regenerative potential for the adsorbents' usage.

REFERENCES

- Abas, S.A., Ismail, M.S., Kamal, M. and Izhar S. (2013): Adsorption Process of Heavy Metals by Low-Cost Adsorbent: A Review. *World Applied Sciences Journal*, 28 (11): 1518-1530.
- Abdus-Salam, N. and Adekola, F.A. (2005): The influence of pH and adsorbent concentration on adsorption of lead and zinc on a natural goethite. *African Journal of Science and Technology*, 6: 55-66.
- Abdus-Salam, N. and Itiola, A.D. (2012): Potential application of termite mound for adsorption and removal of Pb(II) from aqueous solutions. *Journal of Iranian Chemical Society*, 9: 373-382.
- Abdus-Salam, N and Bello, M.O. (2015): Kinetics, thermodynamics and competitive adsorption of lead and zinc ions onto termite mound. *International Journal of Environmental Science and Technology*, 12: 3417-3426.
- Abdus-Salam, N. and Ikudayisi, V.A. (2017): Preparation and characterization of synthesized goethite and goethite-date palm seeds charcoal composite. *Ifè Journal Science*, 19: 99-107.
- Abdus-Salam, N. and Adekola, S.K. (2018): Adsorption studies of zinc(II) on magnetite, baobab (*Adansonia digitata*) and magnetite-baobab composite. *Applied Water Science*, 8: 222.
- Abia, A.A. and Asuquo, E.D. (2006): Lead (II) and nickel (II) adsorption kinetics from aqueous metal solutions using chemically modified and unmodified agricultural adsorbents. *African Journal of Biotechnology*, 5: 1475-1482.
- Adekola, F.A., Abdus-Salam, N. and Abdul-Rauf, L.B. (2011): Removal of Arsenic from aqueous solution by Synthetic Hematite. *Journal of Chemical Society of Nigeria*, 36: 52-58.
- Alhamed, Y.A. and Bamufleh, H.S. (2009): Sulfur removal from model diesel fuel using granular activated carbon from dates' stones activated by $ZnCl_2$. *Fuel*, 88: 87-94.
- Alli, H. and Muhammad, S.K. (2008): Biosorption of crystal violet from water on leaf biomass of *Calotropis procera*. *Journal of Environmental Science and Technology*, 1: 143-150.
- Amer, M.W., Khalili, Fawwaz I., A. and Awwad, A.M. (2010): Adsorption of lead, zinc and cadmium ions on polyphosphate-modified kaolinite clay. *Journal Environmental Chemistry and Ecotoxicology*, 2: 1-8.
- Atkins, P.W. (1995) *Physical Chemistry*, Fifth ed. New York, Oxford University Press, pp 122-124.
- Babarinde, N.A.A. and Babalola, J.O. (2010): The Biosorption of Pb(II) from Solution by Elephant Grass (*Pennisetum purpureum*): Kinetic, Equilibrium, and Thermodynamic Studies. *The Pacific Journal of Science and Technology*, 11: 622-630.
- Bayat, B. (2002): Comparative study of adsorption properties of Turkish fly ashes: I. The case of nickel(II), copper(II) and zinc(II). *Journal of Hazardous Materials*, 95: 251-273.
- Bello, M. O., Abdus-Salam, N., Adekola, F. A. and Pal, U. (2021): Isotherm and kinetic studies of adsorption of methylene blue using activated carbon from ackee apple pods. *Chemical Data Collections*. <https://doi.org/10.1016/j.cdc.2020.100607>
- Bhamare V.S., Kulkarni R. M. and Khan A. A. (2021): Adsorptive removals of pollutants using aerogels and its composites. *Advance in Aerogel Composites for Environmental Remediation*, 171-199.
- Bisht R., Agarwal M. and Singh K. (2016): Heavy metal removal from wastewater using various adsorbents: a review. *Journal of Water Reuse and Desalination*, 7 (4): 387-419.
- Bulut, Y. and Aydin, H. (2006): A kinetics and thermodynamics study of methylene blue adsorption on wheat shells. *Desalination*, 194: 259-267.
- Castaldi, P., Santona, L., Enzo, S. and Melis, P. (2008): Sorption processes and XRD analysis of a natural zeolite exchanged

- with Pb²⁺, Cd²⁺ and Zn²⁺ cations. *Journal of Hazardous Materials*, 156: 428–434.
- Chakraborty, R., Asthana, A., Singh, A. K., Jain, B. and Susan, A. B., (2020): Adsorption of heavy metal ions by various low-cost adsorbents: a review. *International Journal of Environmental Analytical Chemistry*, 1–38.
- Chao, Y., Zhu, W., Yan, B., Lin, Y., Xun, S., Ji, H., Wu, X., Li, H. and Han, C. (2014): Macroporous polystyrene resins as adsorbents for the removal of tetracycline antibiotics from an aquatic environment. *Journal of Applied Polymer Science*, 131: 1–8.
- Chen, S.B., Ma, Y.B., Chen, L. and Xian, K. (2010): Adsorption of aqueous Cd²⁺, Pb²⁺, Cu²⁺ ions by nano-hydroxyapatite: Single- and multi-metal competitive adsorption study. *Geochemical Journal*, 44: 233–239.
- Chen, X. (2015): Modeling of Experimental Adsorption Isotherm Data. *Information*, 6(1): 14–22.
- Chigondo, F. and Nyamunda, B. (2013): Removal of lead (II) and copper (II) ions from aqueous solution by baobab (*Adonnia digitata*) fruit shells biomass. (*IOSR*) *Journal of Applied Chemistry*, 5: 43–50.
- Chowdhury, S. R. (2013): Application of mixed iron oxides in subsurface remediation technologies. London, Ont.: School of Graduate and Postdoctoral Studies, University of Western Ontario. <http://ir.lib.uwo.ca/etd/> (accessed 16 May 2016).
- Crini, G. (2006): Non-conventional low-cost adsorbents for dye removal: A review. *Bioresource Technology*, 97: 1061–1085.
- Emadi, M., Shams, E. and Amini, M.K. (2013): Removal of zinc from aqueous solutions by magnetite silica core-shell nanoparticles. *Journal of Chemistry*, 5: 1-10.
- Foo, K.Y. and Hameed, B.H. (2010): Insights into the modeling of adsorption isotherm systems. *Chemical Engineering Journal*, 156: 2-10.
- Giraldo, L. and Moreno-piraján, J.C. (2013): Synthesis of magnetite nanoparticles and exploring their application in the removal of Pt²⁺ and Au³⁺ ions from aqueous solutions. *European Chemical Bulletin*, 2(7): 445–452.
- Hedström, A. (2001): Ion Exchange of Ammonium in Zeolites: A Literature Review. *Journal of Environmental Engineering*, 127: 673–681.
- Ho, Y.S. and McKay, G. (1998): Kinetic models for the sorption of dye from aqueous solution by wood. *Process Safety and Environmental Protection*, 76: 183–191.
- Ho, Y.S. and McKay, G. (1999): Pseudo-second order model for sorption processes. *Process Biochemistry*, 34: 451–465.
- Inyinbor, A.A., Adekola, F.A., and Olatunji, G.A. (2016): Kinetics, isotherms and thermodynamic modeling of liquid phase adsorption of Rhodamine B dye onto *Raphia hookeri* fruit epicarp. *Water Resources and Industry*, 15: 14–27.
- Jain, C.K. and Sharma, M.K. (2002): Adsorption of Cadmium on Bed Sediments of River Hindon: Adsorption Models and Kinetics. *Water, Air and Soil Pollution*, 137: 1–19.
- Jimoh, T. O., Buoro A.T. and Muriana M. (2012): Utilization of *Blighia sapida* (Akee apple) pod in the removal of lead, cadmium and cobalt ions from aqueous solution. *Journal of Environmental Chemistry and Ecotoxicology*, 4: 178–187.
- Kaya, Y., Aksakal, Ö. and Uzun, H. (2009): Biosorption of lead(II) and zinc(II) from aqueous solutions by nordmann fir (*Abies nordmanniana* (Stev.) Pach. Subsp. *Nordmanniana*) cones. *Acta Chimica Slovenica*, 56: 451–456.
- Kadirvelu, K. and Namasivayam, C. (2003): Activated Carbon from Coconut Corpith as Metal Adsorbent: Adsorption of Cd(II) from Aqueous Solution. *Advances in Environmental Research*, 7: 471-478
- Khodabakhshi, A., Amin, M. M. and Mozaffari, M. (2011): Synthesis of magnetite nanoparticles and evaluation of its efficiency for arsenic removal from simulated industrial wastewater. *Journal of Environmental Health Science and Engineering*, 8: 189-200.
- Liu, Y. and Liu, Y.J. (2008): Biosorption isotherms, kinetics and thermodynamics. *Separation and Purification Technology*, 61: 229–242
- Mohammed, A.K., Ali, S.A., Najem, A.M. and Ghaima, K.K. (2013): Effect of some factors on biosorption of lead by dried leaves of water hyacinth (*Eichhornia crassipes*). *International Journal of Pure Applied Science and Technology*, 17: 72–78.
- Naiya, T.K., Chowdhury, P., Bhattacharya, A.K. and Das, S.K. (2009): Saw dust and neem bark as low-cost natural biosorbent for adsorptive removal of Zn(II) and Cd(II) ions from aqueous solutions. *Chemical Engineering Journal*, 148: 68–79.
- Najim, T.S., Elais, N.J. and Dawood, A.A. (2008): Adsorption of Copper and Iron Using Low Cost Material as Adsorbent. *Journal of Chemistry*, 6(1): 161-168.
- Omar, W. and Al-Itawi, H. (2007): Removal of Pb²⁺ ions from aqueous solutions by adsorption on kaolinite clay. *American Journal of Applied Sciences*, 4(7): 502–507.
- Onundi, Y.B., Mamun, A.A., Al Khatib, M.F. and Ahmed, Y.M. (2010): Adsorption of copper, nickel and lead ions from synthetic

- semiconductor industrial wastewater by palm shell activated carbon. *International Journal of Environmental Sciences and Technology*, 7: 751–758.
- Orumwense, F.F.O. (1996): Removal of Lead from Water by Adsorption on a Kaolinitic Clay. *Journal of Chemical Technology and Biotechnology*, 65: 363–369.
- Ren, J., Bopape, M.F., Setshedi, K., Kitinya, J.O. and Onyango, M.S. (2012): Sorption of Pb(II) and Cu(II) by low-cost magnetic eggshell-Fe₃O₄ powder. *Chemical Industry and Chemical Engineering Quarterly*, 18: 221–231.
- Salami, N. and Adekola, F.A. (2002): A study of sorption of cadmium by goethite in aqueous solution. *Bulletin of the Chemical Society of Ethiopia*, 16: 1–7.
- Sani, U. (2011): Determination of some heavy metals concentration in the tissues of Tilapia and Catfishes. *Biokemistri*, 23: 73–80.
- Sen, T.K., Afroze, S. and Ang, H.M. (2011): Equilibrium, kinetics and mechanism of removal of methylene blue from aqueous solution by adsorption onto pine cone biomass of *Pinus radiata*. *Water, Air and Soil Pollution*, 218: 499–515.
- Senthil Kumar, P., Vincent, C., Kirthika, K. and Sathish Kumar, K. (2010): Kinetics and equilibrium studies of Pb²⁺ ion removal from aqueous solutions by use of nano-silversol-coated activated carbon. *Brazilian Journal of Chemical Engineering*, 27: 339–346.
- Shikuku, V.O., Zanella, R., Kowenje, C.O., Donato, F.F., Bandeira, N.M. G., and Prestes, O.D. (2018): Single and binary adsorption of sulfonamide antibiotics onto iron-modified clay: linear and nonlinear isotherms, kinetics, thermodynamics, and mechanistic studies. *Applied Water Science*, 8(6): 1-12.
- Tchounwou, P.B., Yedjou, C.G., Patlolla, A.K. and Sutton, D.J. (2012): Heavy metal toxicity and the environment. *Molecular, Clinical and Environmental Toxicology*, 101: 1–30.
- Wang, K. and Xing, B. (2002): Adsorption and desorption of cadmium by goethite pretreated with phosphate. *Chemosphere*, 48: 665–670.
- Wang, N., Han, Y., Liu, Y., Bai, T., Gao, H., Zhang, P., Wang, W. and Liu, W. (2012): High-strength hydrogel as a reusable adsorbent of copper ions. *Journal of Hazardous Materials*, 213–214: 258–264.
- Wang, S. and Peng, Y. (2010): Natural zeolites as effective adsorbents in water and wastewater treatment. *Chemical Engineering Journal*, 156: 11–24.
- Zvinowanda, C.M., Okonkwo, J.O., Sekhula, M.M., Agyei, N.M. and Sadiku, R. (2009): Application of maize tassel for the removal of Pb, Se, Sr, U and V from borehole water contaminated with mine wastewater in the presence of alkaline metals. *Journal of Hazardous Materials*, 164: 884–891.